Piezonuclear Fission Reactions in Rocks: Evidences from Microchemical Analysis, Neutron Emission, and Geological Transformation

A. Carpinteri, G. Lacidogna, A. Manuello & O. Borla

Rock Mechanics and Rock Engineering

ISSN 0723-2632

Rock Mech Rock Eng
DOI 10.1007/s00603-011-0217-7

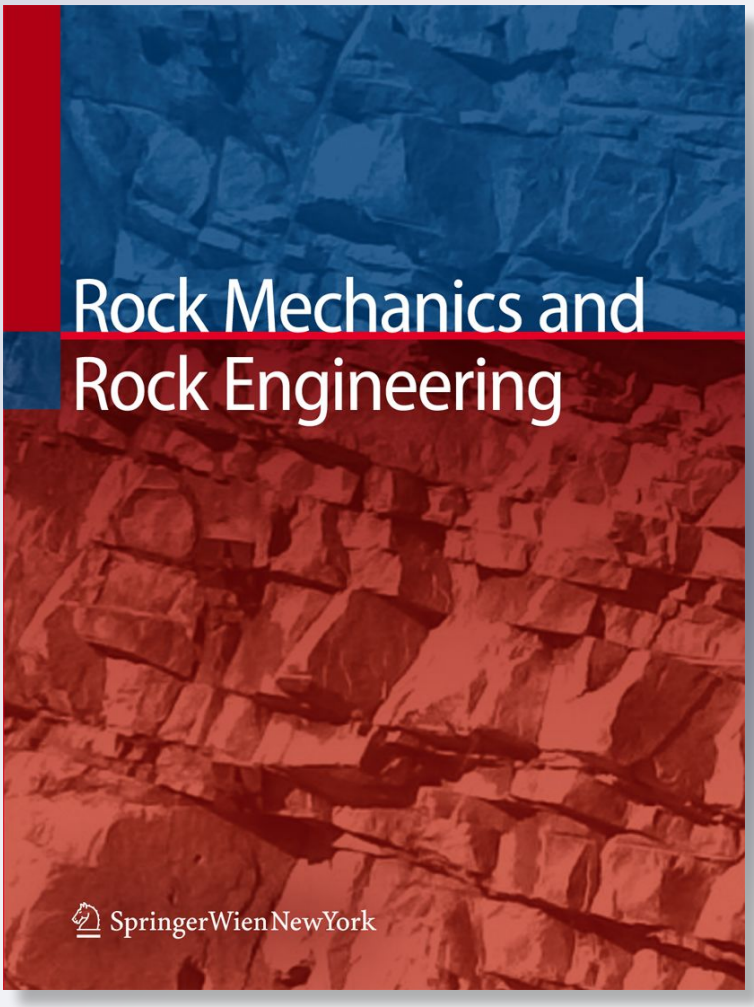

Springer

Rock Mech Rock Eng
DOI 10.1007/s00603-011-0217-7

ORIGINAL PAPER

Piezonuclear Fission Reactions in Rocks: Evidences from Microchemical Analysis, Neutron Emission, and Geological Transformation

A. Carpinteri · G. Lacidogna · A. Manuello · O. Borla

Received: 10 June 2011 / Accepted: 12 December 2011

Abstract Neutron emission measurements, by means of He^3 devices and bubble detectors, were performed during three different kinds of compression tests on brittle rocks: (1) under monotonic displacement control, (2) under cyclic loading, and (3) by ultrasonic vibration. The material used for the tests was Luserna Stone. Since the analyzed material contains iron, our conjecture is that piezonuclear reactions involving fission of iron into aluminum, or into magnesium and silicon, should have occurred during compression damage and failure. This hypothesis is confirmed by the direct evidence of energy dispersive X-ray spectroscopy tests conducted on Luserna Stone specimens. It is also interesting to emphasize that the anomalous chemical balances of the major events that have affected the geomechanical and geochemical evolution of the Earth's crust should be considered as an indirect evidence of the piezonuclear fission reactions considered above.

Keywords Neutron emission · Piezonuclear reactions · Rocks crushing failure · Energy dispersive X-ray spectroscopy · Plate tectonics · Element evolution

1 Introduction

We deal with a new topic in the scientific literature: piezonuclear neutron emissions from brittle rock specimens under mechanical loading. The phenomenon is analyzed from an experimental point of view. In the scientific community, some studies have been already conducted on the different forms of energy emitted during the failure of brittle materials. They are based on the signals captured by the acoustic emission measurement systems, or on the detection of the electromagnetic charge. On the other hand, only very recently piezonuclear neutron emissions from very brittle rock specimens in compression have been discovered (Carpinteri et al. 2009, 2010a; Cardone et al. 2009). Piezonuclear fission reactions consist of a new nuclear phenomenon, produced by physical causes such as pressure, fracture or cavitation, and from which neutrons can be produced without gamma emission. This physical phenomenon could be the signature of a new physics of nuclear interactions, as it is theoretically and experimentally discussed in the literature (Cardone and Mignani 2004, 2006, 2007; Cardone et al. 2009).

In this paper, we present the original experimental tests, using He^3 neutron detectors and bubble-type BD thermodynamic neutron detectors, performed on brittle rock test specimens. We carried out three different kinds of compression tests: (1) under monotonic displacement control, (2) under cyclic loading, and (3) by ultrasonic solicitations. Similar to the preliminary piezonuclear experiments presented in (Carpinteri et al. 2009, 2010a; Cardone et al. 2009), the material used for the tests is non-radioactive Luserna Stone, a metamorphic rock deriving from a granitoid protolith. In these new tests, cylindrical specimens with different size and slenderness are used to assess neutron emissions related to specimens with very brittle behavior. The compression tests were performed at the Fracture Mechanics Laboratory of the Politecnico of Torino, while the ultrasonic tests at the Medical and Environmental Physics Laboratory of the University of Torino.

A. Carpinteri (✉) · G. Lacidogna · A. Manuello · O. Borla
Department of Structural Engineering and Geotechnics, Politecnico di Torino, Corso Duca degli Abruzzi 24, 10129 Turin, Italy
e-mail: alberto.carpinteri@polito.it

O. Borla
Istituto Nazionale di Fisica Nucleare, INFN sez. Torino Via Pietro Giuria 1, 10125 Turin, Italy

Published online: 28 January 2012

For specimens of larger dimensions characterized by a brittle behavior, neutron emissions, detected by He^3, were found to be of about one order of magnitude higher than the ordinary natural background level at the time of the catastrophic failure. As regards test specimens with more ductile behavior, neutron emissions significantly higher than the background level were also found. These piezonuclear reactions are due to the different modalities of energy release during the tests. For specimens with sufficiently large size and slenderness, a relatively large energy release is expected, and hence a higher probability of neutron emissions at the time of failure. Furthermore, during compression tests under cyclic loading, an equivalent neutron dose, analyzed by neutron bubble detectors, about two times higher than the ordinary background level was found at the end of the test.

Finally, by using an ultrasonic horn suitably joined with the specimen, an ultrasonic test was carried out on a Luserna Stone specimen to produce continuing vibration at 20 kHz. Three hours after the beginning of the test, an equivalent neutron dose about three times higher than the background level was found. The results of this study are reported in (Carpinteri et al. 2010b, 2011).

Piezonuclear reactions with neutron emissions were obtained for the first time in liquids containing iron chloride or iron nitrate subjected to ultrasounds and cavitation (Cardone and Mignani 2007; Cardone et al. 2009). In the experiments on liquid solutions (Cardone and Mignani 2007; Cardone et al. 2009), aluminum atoms appeared at the end in a final quantity as large as about seven times the small initial quantity (Cardone et al. 2009). By analogy with the case of piezonuclear reactions in liquids, a factor to be taken into account is the composition of the materials in which piezonuclear reactions may be produced. Since the Luserna Stone contains iron (around 3% of Fe_2O_3), it was supposed that piezonuclear reactions involving fission of iron into aluminum, or into magnesium and silicon, should have occurred during compression of the rock specimens.

Even small deviations from classical assumptions, e.g., from the concept of average binding energy per nucleon, could explain these new phenomena. It is not even necessary to resort to dynamical resonance or to tunneling effects. It would suffice to assume a weak section within the nucleus, as it analogously happens in very hard and strong rocks that nevertheless cleave under very low stresses.

Therefore, energy dispersive X-ray spectroscopy (EDS) was performed on different samples of external or fracture surfaces belonging to specimens used in the preliminary piezonuclear tests (Carpinteri et al. 2010c). For each sample, different measurements of the same crystalline phases (phengite or biotite) were performed to get average information of the chemical composition and to detect possible piezonuclear transmutations from iron to lighter elements. The samples were carefully chosen to investigate and compare the same minerals before and after the crushing failure. Phengite and biotite that are rather common in the Luserna Stone (20 and 2%, respectively) were considered owing to the high iron concentration in their chemical compositions. The results of EDS analyses show that, on the fracture surface samples, a considerable reduction in the iron content ($\sim$25%) is counterbalanced by a nearly equal increase in Al, Si, and Mg concentrations.

The present natural abundances of aluminum ($\sim$8%) and silicon (28%), and scarcity of iron ($\sim$4%) in the continental Earth's crust are possibly due to the piezonuclear fission reactions considered above. These reactions would be activated where the environment conditions (pressure and temperature) are particularly severe, and mechanical phenomena of fracture, crushing, fragmentation, comminution, erosion, friction, etc., may occur.

From this point of view, piezonuclear reactions, induced by the sliding of faults and plate subduction phenomena at the Earth' crust scale, could imply the different mineral reservoir localizations on the Earth's surface and the most significant chemical element evolutions over the past 4.57 Gyrs (Earth's life time). The geomechanical and geochemical evidences shown in this paper involve the most abundant elements in the Earth's continental crust such as Si, Al, Mg, Fe, Ca, K, and Na. Therefore the plate tectonics, the related plate collisions, and the subduction phenomena are useful to understand not only the morphology of our planet, but also its compositional evolution (Carpinteri and Manuello 2010).

2 Neutron Emission Detection Techniques

Since neutrons are electrically neutral particles, they cannot directly produce ionization in a detector, and therefore cannot be directly detected. This means that neutron detectors must rely upon a conversion process where an incident neutron interacts with a nucleus to produce a secondary charged particle. These charged particles are then detected, and from them the neutron's presence is deduced. For an accurate neutron evaluation, an He^3 proportional counter and a set of passive neutron detectors, based on the superheated bubble detection technique, insensitive to electromagnetic noise, were employed.

2.1 He^3 Proportional Counter

The He^3 detector used in the tests is an He^3 type (Xeram, France) with electronics of preamplification, amplification, and discrimination directly connected to the detector tube.

The detector is powered with high voltage power supply (about 1.3 kV) via NIM (Nuclear Instrument Module). The logic output producing the TTL (transistor–transistor logic) pulses is connected to an NIM counter. The logic output of the detector is enabled for analog signals exceeding 300 mV. This discrimination threshold is a consequence of the sensitivity of the He^3 detector to the gamma rays ensuing neutron emission in ordinary nuclear processes. This value has been determined by measuring the analog signal of the detector by means of a Co-60 gamma source. The detector is also calibrated at the factory for the measurement of thermal neutrons; its sensitivity is 65 cps/n_{thermal} ($\pm 10\%$ declared by the factory), i.e., the flux of thermal neutrons was one thermal neutron/s cm^2, corresponding to a count rate of 65 cps.

2.2 Neutron Bubble Detectors

A set of passive neutron detectors insensitive to electromagnetic noise and with zero gamma sensitivity was used. The dosimeters, based on superheated bubble detectors (BTI, ON, Canada) (Bubble Technology Industries 1992), are calibrated at the factory against an AmBe (Americium-Beryllium) source in terms of NCRP38 (National Council on Radiation Protection and Measurements 1971). Bubble detectors are the most sensitive, accurate neutron dosimeters available that provide instant visible detection and measurement of neutron dose. Each detector is composed of a polycarbonate vial filled with elastic tissue equivalent polymer, in which droplets of a superheated gas (Freon) are dispersed. When a neutron strikes a droplet, the latter immediately vaporizes, forming a visible gas bubble trapped in the gel. The number of droplets provides a direct measurement of the equivalent neutron dose with an efficiency of about 20%. These detectors are suitable for neutron dose measurements in the energy range of thermal neutrons ($E = 0.025$ eV, BDT type) and fast neutrons ($E > 100$ keV, BD-PND type).

3 Experimental Set-Up

3.1 Compression Tests Under Monotonic Displacement Control

Similar to the preliminary piezonuclear tests presented in (Carpinteri et al. 2009, 2010a; Cardone et al. 2009), the material used for the tests is non-radioactive Luserna Stone. In these new experiments, cylindrical specimens with different size and slenderness are used to assess neutron emissions related to specimens with very brittle or catastrophic failure (Carpinteri 1989, 1990). Neutron emissions were measured on nine Luserna Stone cylindrical specimens, of different size and shape (Fig. 1; Table 1), denoted with P1, P2,…, P9. The tests were carried out by means of a servo-hydraulic press, with a maximum capacity of 1,800 kN, working by a digital type electronic control unit. The management software was TESTXPER-TII by Zwick/Roel (Zwick/Roel Group, Ulm, Germany), while the mechanical parts were manufactured by Baldwin (Instron Industrial Products Group, Grove City, PA, USA). The force applied was determined by measuring the pressure in the loading cylinder by means of a transducer. The margin of error in the determination of the force is 1%, which makes it a class 1 mechanical press. The specimens

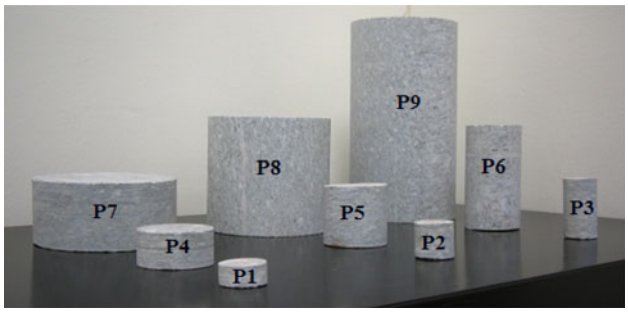

Fig. 1 Luserna Stone cylindrical specimens, by varying slenderness and size scale

Table 1 Characteristics of compression tests under monotonic displacement control on Luserna Stone specimens

Granite specimen	Geometry of the specimen			Displacement velocity (mm/s)	Peak load (kN)	Time at the peak load (s)
	D (mm)	H (mm)	$\lambda = H/D$			
P1	28	14	0.5	0.001	52.19	735.0
P2	28	28	1	0.001	33.46	1,239.0
P3	28	56	2	0.001	41.28	1,089.0
P4	53	25	0.5	0.001	129.00	960.0
P5	53	50	1	0.001	139.10	2,460.0
P6	53	101	2	0.001	206.50	1,180.0
P7	112	60	0.5	0.01	1,099.30	231.3
P8	112	112	1	0.01	1,077.10	263.5
P9	112	224	2	0.01	897.80	218.6

were arranged with the two smaller surfaces in contact with the press platens, without coupling materials in-between, according to the testing modalities known as "test by means of rigid platens with friction". The tests were performed under monotonic loading, with the planned displacement velocities ranging from 0.001 to 0.01 mm/s.

The He^3 neutron detector was switched on at least 1 h before the beginning of each compression test to reach the thermal equilibrium of electronics, and to make sure that the behavior of the devices was stable with respect to intrinsic thermal effects. The detector was placed in front of the test specimen at a distance of 20 cm and it was enclosed in a polystyrene case of 10 cm of thickness to avoid "spurious" signals coming from impact and vibration.

A relative measurement of natural neutron background was performed to assess the average background affecting data acquisition in experimental room condition. The He^3 device was positioned in the same condition of the experimental set-up and the background measures were performed fixing at 60 s the acquisition time, during a preliminary period of more than 3 h, for a total number of 200 counts. The average measured background level ranged from $(3.17 \pm 0.32) \times 10^{-2}$ to $(4.74 \pm 0.46) \times 10^{-2}$ cps (see Table 2).

3.2 Compression Test Under Cyclic Loading

A Luserna Stone specimen ($D = 53$ mm, $H = 53$ mm, $\lambda = 1$) was used. The cyclic loading was programmed at a frequency of 2 Hz and with a load excursion from a minimum load of 10 kN to a maximum of 60 kN. With respect to the tests performed under monotonic displacement control, neutron emissions from compression test under cyclic loading were performed by using neutron bubble detectors. Due to their isotropic angular response, three BDT and three BD-PND detectors were positioned at a distance of about 5 cm, all around the specimen. The detectors were previously activated, unscrewing the protection cap, to reach the suitable thermal equilibrium, and they were kept active throughout the test duration. Furthermore, a BDT and a BD-PND detector were used as background control during the test.

Table 2 Compression tests under monotonic displacement control

Granite specimen	D (mm)	$\lambda = H/D$	Average neutron background (10^{-2} cps)	Count rate at the neutron emission (10^{-2} cps)
P1	28	0.5	3.17 ± 0.32	8.33 ± 3.73
P2	28	1	3.17 ± 0.32	Background
P3	28	2	3.17 ± 0.32	Background
P4	53	0.5	3.83 ± 0.37	Background
P5	53	1	3.84 ± 0.37	11.67 ± 4.08
P6	53	2	4.74 ± 0.46	25.00 ± 6.01
P7	112	0.5	4.20 ± 0.80	Background
P8	112	1	4.20 ± 0.80	30.00 ± 11.10
P9	112	2	4.20 ± 0.80	30.00 ± 10.00

Neutron emissions experimental data on Luserna Stone specimens

Fig. 2 The Luserna Stone specimen connected to the ultrasonic horn. The ultrasonic apparatus (Bandelin HD 2200) consists of a generator that converts electrical energy to 20 kHz ultrasound, and of a transducer that switches this energy into mechanical longitudinal vibration of the same frequency

3.3 Ultrasonic Test

A Luserna Stone specimen ($D = 53$ mm, $H = 100$ mm, $\lambda = 2$) was connected to the ultrasonic horn by a glued screw inserted in a 5-mm deep hole (Fig. 2). This kind of connection was made to achieve a resonance condition, considering the speed of sound in Luserna Stone, and the length of the specimen. Ultrasonic irradiation of the specimen was carried out for 3 h. After the switching on of the transducer, 10% of the maximum power was reached in 20 min. Successively, the transducer power increased to 20% after 1 h, and next reached a maximum level of about 30% after 2 h. Then, the transducer worked on the same power condition up to the end of the test.

4 Experimental Results

4.1 Compression Tests Under Monotonic Displacement Control

Additional background measurements were repeated before each test, fixing an acquisition time of 60 s, up to the

assessment of no significant variation in natural background. Neutron measurements of specimens P2, P3, P4, and P7 yielded values comparable with the ordinary natural background, whereas in specimens Pl and P5 the experimental data exceeded the background value by about four times. Instead, for specimen P6, P8 and P9, the neutron emissions achieved values about one order of magnitude higher than ordinary background. In Fig. 3, the load versus time diagram and the neutron count rate evolution for specimens P6, P8, and P9 are shown. In Table 2, experimental data concerning compression tests on the nine Luserna Stone specimens are summarized.

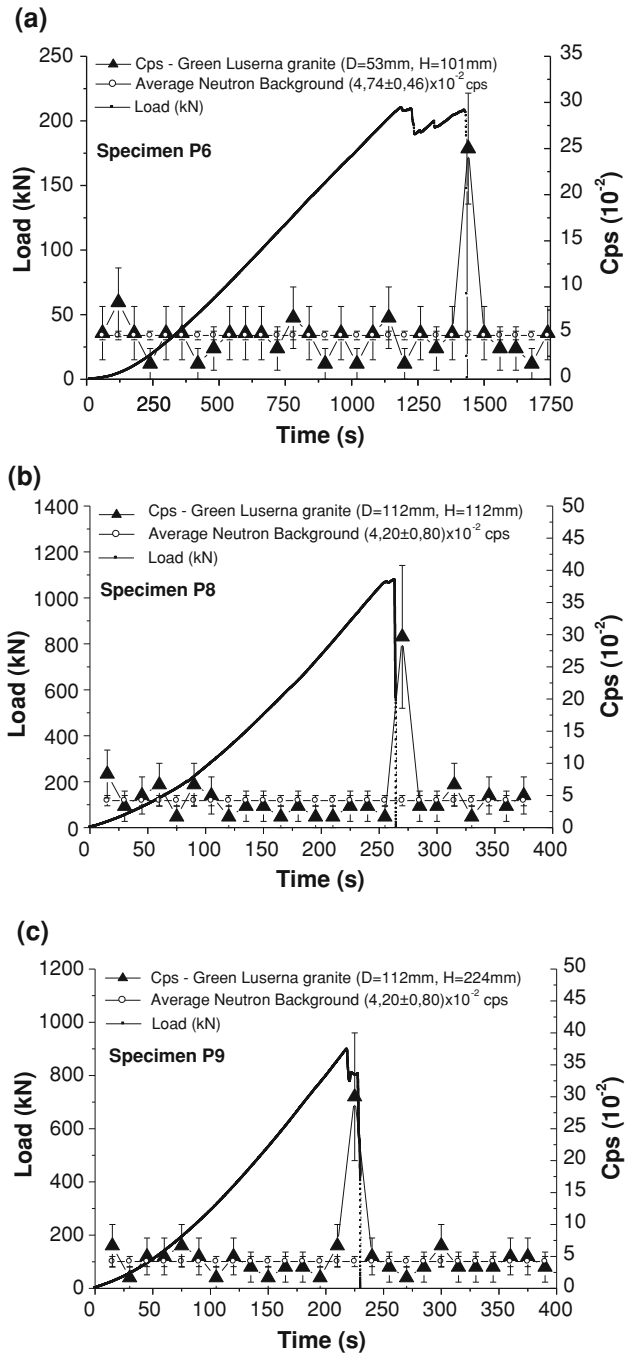

Fig. 3 Specimens P6, P8, and P9. Load versus time diagrams, and neutron emissions count rate

The preliminary experimental results described above and reported in (Carpinteri et al. 2009, 2010a; Cardone et al. 2009) are confirmed by those obtained from compression tests on the cylindrical specimens. Neutron emissions related to specimens with very brittle or catastrophic failure result to be larger by about one order of magnitude than the ordinary background (see Fig. 3).

The maximum neutron emissions were obtained from test specimens exceeding a certain volume threshold: 360 cm^3 for the prismatic specimens, and 233 cm^3 for the cylindrical specimens. The experimental results show that a volume approximately exceeding 200 cm^3, combined with the extreme brittleness of the tested material, represents a threshold value for a neutron emission of about one order of magnitude higher than the ordinary background.

In addition, the experimental results seem to demonstrate that neutron emissions follow an anisotropic and impulsive distribution from a specific zone of the specimen. It is a matter of fact that the neutron flux and consequently neutron dose are inversely proportional to the square of the distance from the source. For these reasons, the He^3 device could have underestimated neutron flux intensity. A possible solution for avoiding underestimated data acquisition is an experimental measurement by using more than one He^3 detector and more bubble dosimeters placed around the test specimens.

4.2 Compression Test Under Cyclic Loading

Droplets counting was performed every 12 h and the equivalent neutron dose was calculated. In the same way, the natural background was estimated by means of the two bubble dosimeters used for assessment. The ordinary background was found to be (13.98 ± 2.76) nSv/h.

In Fig. 4, neutron equivalent dose variation, evaluated during the cyclic compression test, is reported. An increment of more than twice with respect to the background level was detected at specimen failure. No significant variations in neutron emissions were observed before the failure. The equivalent neutron dose, at the end of the test, was (28.74 ± 5.75) nSv/h.

4.3 Ultrasonic Test

Ultrasonic oscillation was generated by a high-intensity ultrasonic horn (Bandelin HD 2200) working at 20 kHz. The device guarantees constant amplitude (ranging from 10 to 100%) independently of changing conditions within the sample. The apparatus consists of a generator that converts

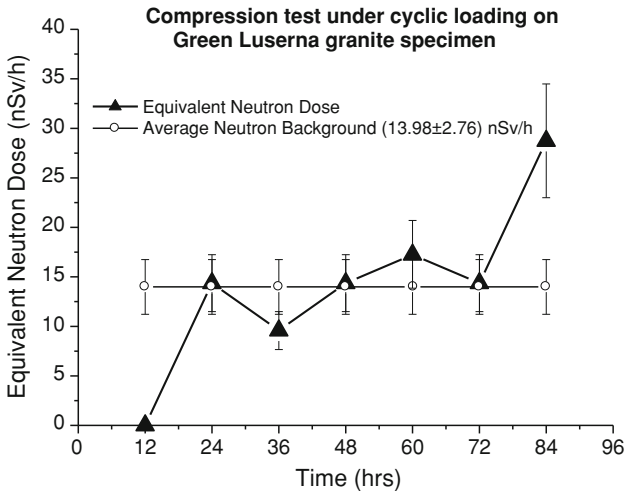

Fig. 4 Compression test under cyclic loading. Equivalent neutron dose variation on Luserna Stone specimen

electrical energy to 20 kHz ultrasounds, and of a transducer that switches this energy into mechanical longitudinal vibration at the same frequency.

The ultrasonic test on Luserna Stone specimen ($D = 53$ mm, $H = 100$ mm, $\lambda = 2$) was carried out at the Medical and Environmental Physics Laboratory of Experimental Physics Department of the University of Torino. A relative natural background measurement was performed by means of the He^3 detector for more than 6 h. The average natural background was of $(6.50 \pm 0.85) \times 10^{-3}$ cps, for a corresponding thermal neutron flux of $(1.00 \pm 0.13) \times 10^{-4}$ n_{thermal} cm^{-2} s^{-1}. This natural background level, lower than the one calculated during the compression tests at the Fracture Mechanics Laboratory of the Politecnico of Torino, is in agreement with the location of the experimental Physics Laboratory, which is three floors below the ground level.

During the ultrasonic test, the specimen temperature was monitored by using a multimeter/thermometer (Tektronix mod. S3910). The temperature reached 50°C after 20 min, and then increased up to a maximum level of 100°C at the end of the ultrasonic test. In Fig. 5, the neutron emissions detected are compared with the transducer power trend and the specimen temperature. A significant increment in neutron activity after 130 min from the beginning of the test was measured. At this time, the transducer power reached 30% of the maximum, with a specimen temperature of about 90°C. Some neutron variations were detected during the first hour of the test, but they may be due to ordinary fluctuations of natural background. At the switching off of the sonotrode, the neutron activity decreased to the typical background value.

5 Compositional and Microchemical Evidence of Piezonuclear Fission Reactions in the Rock Specimens

Energy dispersive X-ray spectroscopy was performed on different samples of external or fracture surfaces, belonging to the same specimens in Luserna Stone used in the preliminary piezonuclear tests by Carpinteri et al. (2009, 2010a) and Cardone et al. (2009). The tests were conducted to correlate the neutron emission from the Luserna Stone with the variations in rock composition due to brittle failure of the granitic gneiss specimens. These analyses lead to get averaged information of the mineral chemical composition

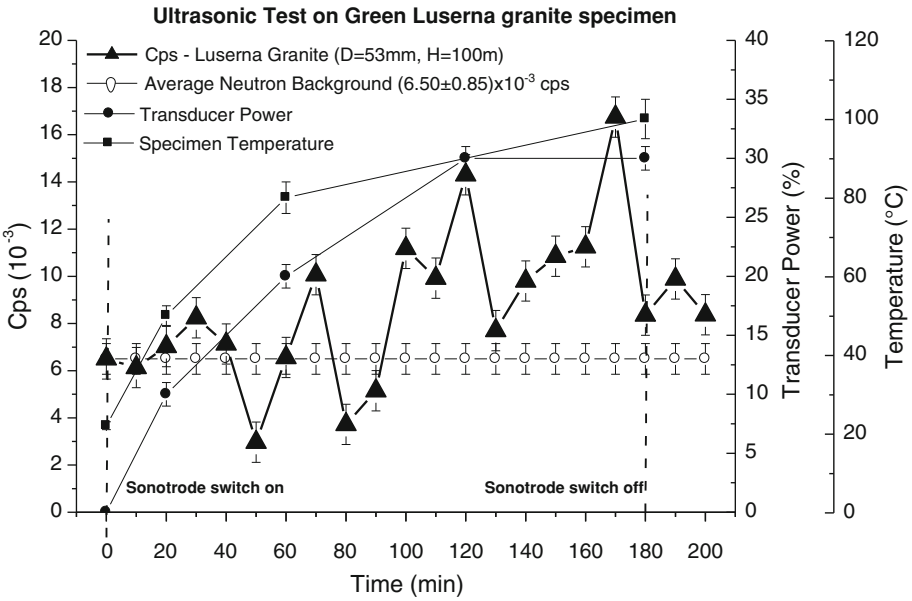

Fig. 5 Ultrasonic test. Neutron emissions compared with the specimen temperature, and with the transducer power trend

and to detect possible piezonuclear transmutations from iron to lighter elements. The quantitative elemental analyses were performed by a ZEISS Supra 40 Field Emission Scanning Electron Microscope (FESEM) equipped with an Oxford X-ray microanalysis. The samples were carefully chosen to investigate and compare the same crystalline phases both before and after the crushing failure.

In particular, two crystalline phases, phengite and biotite, were considered due to their high iron content and relative abundances in the Luserna Stone (20 and 2%, respectively) (Vola and Marchi 2010).

Luserna "Stone" is a leucogranitic orthogneiss, probably from the Lower Permian Age that outcrops in the Luserna-Infernotto basin (Cottian Alps, Piedmont) at the border between the Turin and Cuneo provinces (northwestern Italy) (Sandrone et al. 1993). Characterized by a micro "Augen" texture, it is gray-greenish or locally pale blue in color. Geologically, Luserna Stone pertains to the Dora-Maira Massif (Sandrone et al. 1993; Compagnoni et al. 1983) that represents a part of the ancient European margin annexed to the Cottian Alps during Alpine orogenesis. From a petrographic point of view, it is the metamorphic result of a late-Ercinian leucogranitic rock transformation (Vola and Marchi 2010; Compagnoni et al. 1983). The Luserna Stone has a sub-horizontal attitude, with a marked fine-grained foliation that is mostly associated with visible lineation. The mineralogical composition includes K-feldspar (10–25 Wt. %), quartz (30–40 Wt. %), albite (15–25 Wt. %) and phengite (10–20 Wt. %), and subordinated biotite, chlorite, zoisite, and/or clinozoisite/epidote (less then 5%). In addition to common accessory phases (ores, titanite, apatite, and zircon), tourmaline, carbonates, rare axinite, and frequent fluorite are present (Vola and Marchi 2010; Sandrone et al. 2004).

In consequence of Luserna Stone being a very heterogeneous rock, and in order to assess mass percentage variations in chemical elements such as Fe, Al, Si, and Mg, the EDS analyses have been focused on two crystalline phases: phengite and biotite. These two minerals of granitic gneiss that are quite common in the Luserna Stone (20 and 2%, respectively) show a mineral chemistry in which the iron content is largely diffused (see Fig. 6a, b).

In Fig. 7a, two thin sections obtained from the external surfaces of an integer and uncracked portion of one of the tested specimens are shown. The thin sections, finished with a standard petrographic polishing procedure, present a rectangular geometry (45×27 mm^2) and are 30-μm thick. In Fig. 7b, two portions of fracture surfaces taken from the tested specimen are shown. For the EDS analyses, several phengite and biotite sites were localized on the surface of the thin sections and on the fracture surfaces. Sixty measurements of phengite crystalline phase and 30 of biotite were selected and analyzed. In Fig. 8a, b, two electron microscope images of phengite and biotite sites, the first in the external sample (thin section 1) and the second on the fracture surface (fracture surface 2), are shown.

5.1 EDS Results for Phengite

In Fig. 9a, b, the results for the Fe concentrations obtained from the measurements on phengite crystalline phase are shown. Of these measurements, 30 were carried out on the polished thin sections as representatives of the external surface samples, whereas the other 30 measurements were carried out on fracture surfaces. It can be observed that the distribution of Fe concentrations for the external surfaces, represented in the graph by squares, show an average value of the distribution (calculated as the arithmetic mean value) equal to 6.20%. In the same graph, the distribution of Fe concentrations on the fracture samples (indicated by triangles) shows significant variations. It can be seen that the

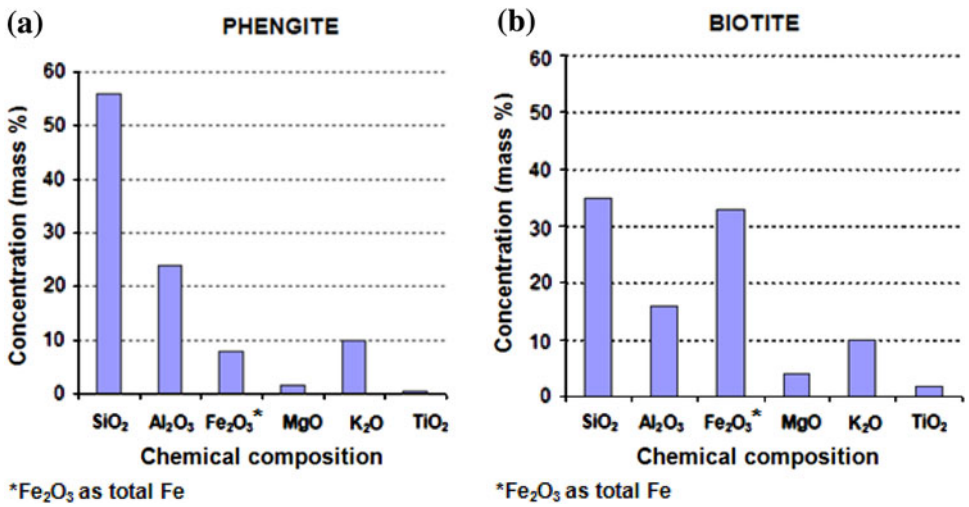

Fig. 6 **a** The chemical composition of phengite includes: SiO_2 (~56%), Al_2O_3 (~24%), Fe_2O_3 and FeO (~8%) MgO (~1.5%), Na_2O (~0.2%), and K_2O (~10%). **b** The chemical composition of biotite includes: SiO_2 (~35%), Al_2O_3 (~16%), Fe_2O_3 and FeO (~33%), MgO (~3.5%), TiO_2 (~1.5%), and K_2O (~10%)

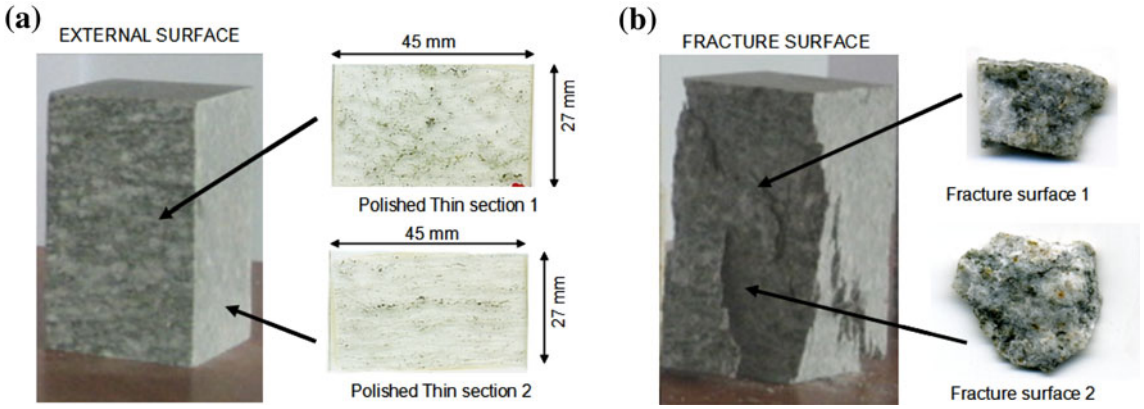

Fig. 7 **a** Polished thin sections obtained by the external surface of an integer and not fractured portion of the tested specimens (Carpinteri et al. 2009, 2010a; Cardone et al. 2009). **b** Fracture surface belonging to the tested specimens (Carpinteri et al. 2009, 2010a; Cardone et al. 2009)

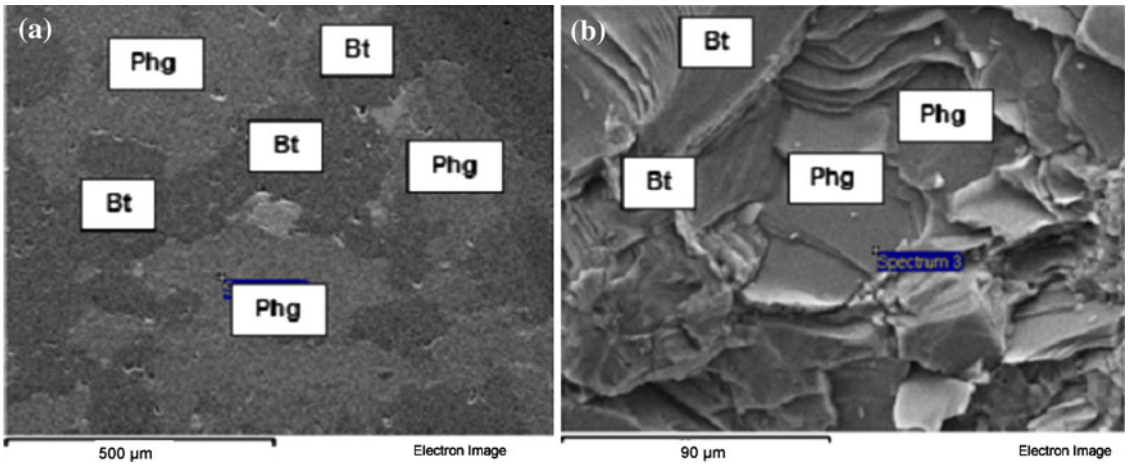

Fig. 8 FESEM images of phengite and biotite in the case of **a** external and **b** fracture sample

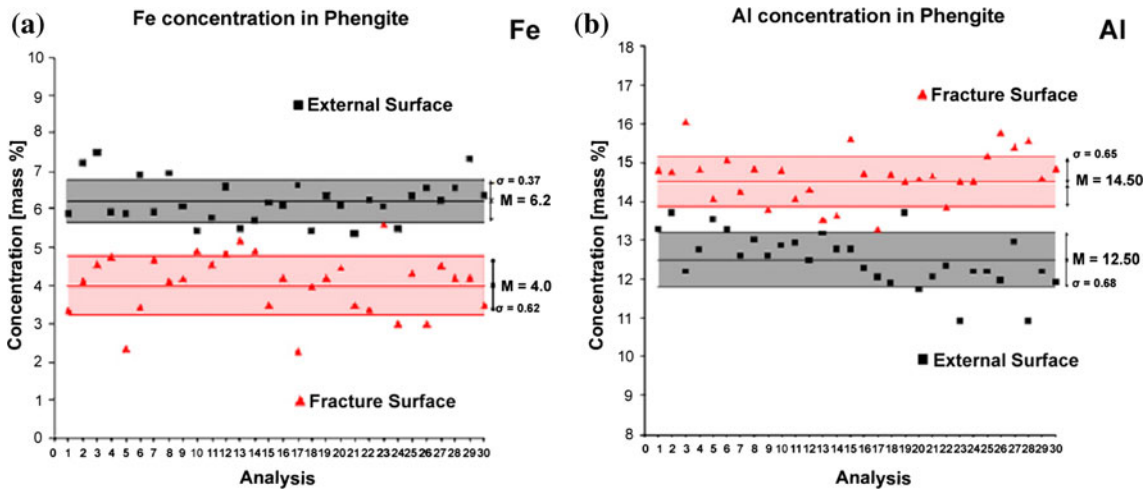

Fig. 9 Fe and Al concentrations in phengite: **a** Fe concentrations on external surfaces (*squares*) and on fracture surfaces (*triangles*). The Fe decrease considering the two mean values of the distributions is equal to 2.20%. **b** Al concentrations on external surfaces (*squares*) and on fracture surfaces (*triangles*). The Al increase, considering the two mean values of the distributions, is equal to 2.0%

mean value of the distribution of measurements performed on fracture surfaces is equal to 4.00% and considerably lower than the mean value of external surface measurements (6.20%). It is also interesting to note that the two Fe value distributions are separated by at least two standard deviations ($\sigma = 0.37$ in the case of external surfaces and $\sigma = 0.52$ in the case of fracture surfaces).

The iron decrease, considering the mean values of the distributions of phengite composition, is about 2.20%. This iron content reduction corresponds to a relative decrease of 35% with respect to the previous Fe content (6.20% in phengite). Similarly to Fig. 9a, in b the Al mass percentage concentrations are considered in both the cases of external and fracture surfaces. For Al contents, the observed variations show a mass percentage increase approximately equal to that of Fe (compare Fig. 9a, b). The average increase in the distribution, corresponding to the fracture surfaces (indicated by triangles), is about 2.00% of the phengite composition. The average value of Al concentrations changes from 12.50% on the external surface to 14.50% on the fracture surface. The relative increase in Al content is equal to 16%.

The evidence emerging from the EDS analyses that the two values for the iron decrease (−2.20%) and for the Al increase (+2.00%) are approximately equal is really impressive. This fact is even more evident considering the trends of the other chemical elements constituting the mineral chemistry (excluding H and O) in phengite, because no appreciable variations can be recognized between the average values (Carpinteri et al. 2010c).

5.2 EDS Results for Biotite

In Fig. 10a–d, the results for Fe, Al, Si, and Mg concentrations measured on 30 acquisition points of biotite crystalline phase are shown. These measurements were selected on the polished thin sections as representatives of the uncracked material samples (15 measurements) and on the fracture surfaces (15 measurements). It can be observed that the distribution of Fe concentrations for the external

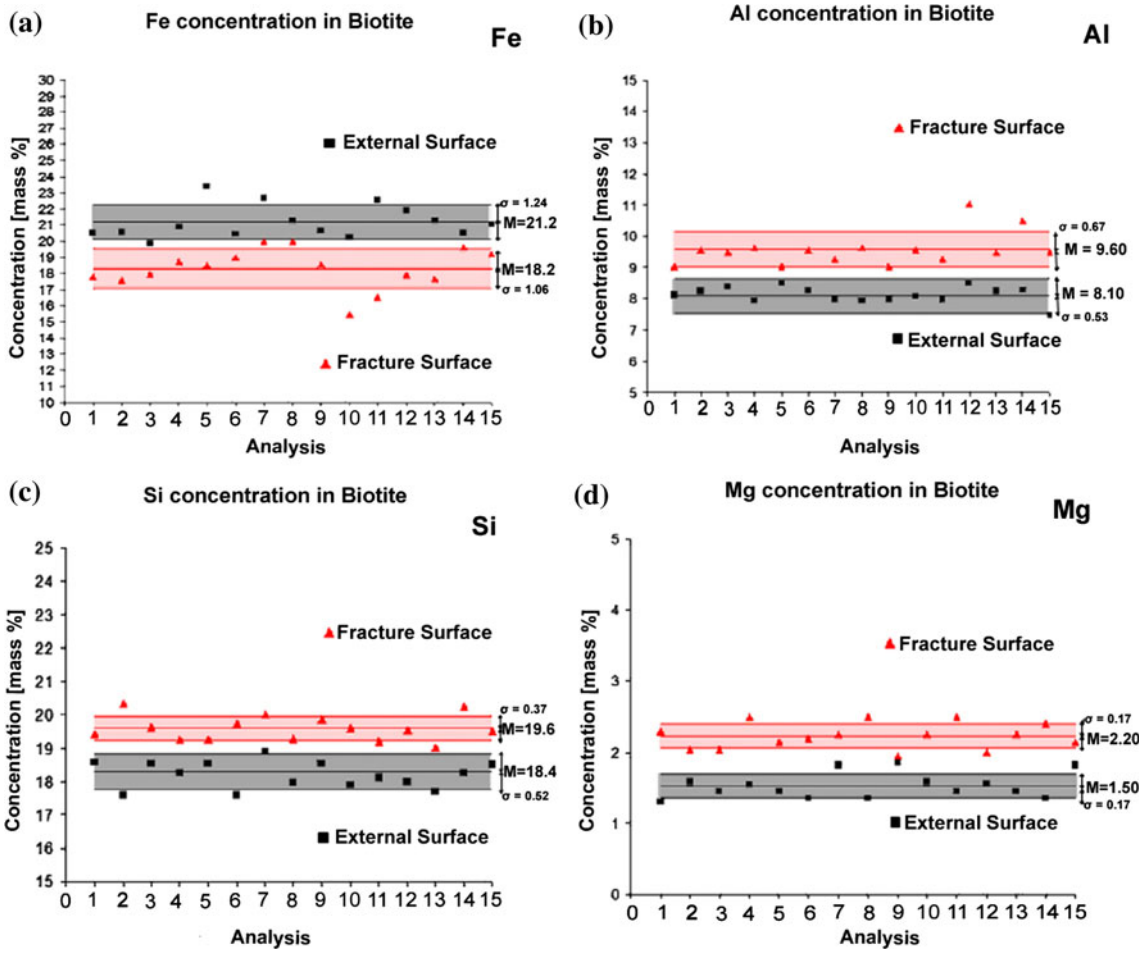

Fig. 10 Fe (**a**), Al (**b**), Si (**c**), and Mg (**d**) concentrations in biotite are reported for external and fracture surfaces. The iron decrease (−3.00%) in biotite is counterbalanced by an increase in aluminum (+1.50%), silicon (+1.20%), and magnesium (+0.70%). In the case of the other elements, no appreciable variations can be recognized between the external and the fracture samples (Carpinteri et al. 2010c)

surfaces, represented in Fig. 10a by squares, shows an average value of the distribution (calculated as the arithmetic mean value) equal to 21.20%. On the other hand, considering in the same graph the distribution of Fe concentrations on fracture samples (indicated by triangles), it can be seen that the mean value drops to 18.20%. In this case, the iron decrease, considering the mean values of the distributions of biotite composition, is about 3.00%. This iron content reduction (−3.00%) corresponds to a relative decrease of 14% with respect to the previous Fe content (21.20% in biotite). Similar to Fig. 10a, in b, the Al mass percentage concentrations are considered in both cases of external and fracture samples. For Al contents, the observed variations show an average increase of about 1.50% in the biotite composition. The average value of Al concentrations changes from 8.10% on the external surface to 9.60% on the fracture surface, with a relative increase in Al content equal to 18%. In Fig. 10c, d, it is shown that, in the case of biotite, also Si and Mg contents present considerable variations. Figure 10c shows that the mass percentage concentration of Si changes from a mean value of 18.40% (external surface) to a mean value of 19.60% (fracture surface) with an increase of 1.20%. Similarly in Fig. 10d, the Mg concentration distributions show that the mean value of Mg content changes from 1.50% (external surface) to 2.20% (fracture surface). Therefore, the iron decrease (−3.00%) in biotite is counterbalanced by an increase in aluminum (+1.50%), silicon (+1.20%), and magnesium (+0.70%) (Carpinteri et al. 2010c).

6 Piezonuclear Reactions: from the Laboratory to the Earth Scale

From the results shown in the previous sections and the experimental evidence reported in recent papers (Carpinteri et al. 2009, 2010a, c; Cardone et al. 2009), it can be clearly seen that piezonuclear reactions are possible in inert non-radioactive solids.

From the EDS results on fracture samples, the evidences of Fe and Al variations on phengite (Fig. 9) lead to the conclusion that the piezonuclear reaction:

$$\mathrm{Fe}_{26}^{56} \rightarrow 2\mathrm{Al}_{13}^{27} + 2 \text{ neutrons}, \quad (1)$$

should have occurred (Carpinteri et al. 2009, 2010a, c; Cardone et al. 2009). Moreover, considering the evidences for the biotite content variations in Fe, Al, Si, and Mg (Fig. 10), it is possible to conjecture that another piezonuclear reaction, in addition to (1), should have occurred during the piezonuclear tests (Carpinteri et al. 2009, 2010a, c; Cardone et al. 2009):

$$\mathrm{Fe}_{26}^{56} \rightarrow \mathrm{Mg}_{12}^{24} + \mathrm{Si}_{14}^{28} + 4 \text{ neutrons}. \quad (2)$$

Taking into account that granite is a common and widely occurring type of intrusive, Sialic, igneous rock, and that it is characterized by an extensive concentration in the rocks that make up the Earth's crust (∼60% of the Earth's crust), the piezonuclear fission reactions expressed above can be generalized from the laboratory to the Earth's crust scale, where mechanical phenomena of brittle fracture, due to fault collision and subduction, take place continuously in the most seismic areas. This hypothesis seems to find surprising evidence and confirmation from both the geomechanical and the geochemical points of view (Carpinteri and Manuello 2010). The neutron emissions involved in piezonuclear reactions can be detected not only in laboratory experiments, as shown in this paper, and in (Carpinteri et al. 2009, 2010a; Cardone et al. 2009), but also at the Earth's crust scale. Recent neutron emission detections by Kuzhevskij et al. (Kuzhevskij et al. 2003a, b) have led to consider also the Earth's crust, in addition to cosmic rays, as being a relevant source of neutron flux variations.

Neutron emissions measured near the Earth's surface exceeded the neutron background by about three orders of magnitudes in correspondence to seismic activity and rather appreciable earthquakes (Volodichev et al. 2000). This relationship between the processes in the Earth's crust and neutron flux variations has allowed increasing tectonic activity to be detected and methods for short-term prediction and monitoring of earthquakes to be developed (Kuzhevskij et al. 2003a, b). Neutron flux variations, in correspondence to seismic activity, may be evidence of changes in the chemical composition of the crust, as a result of piezonuclear reactions.

The present natural abundances of aluminum (∼8%), silicon (28%) and magnesium (1.3%) and scarcity of iron (∼4%) in the continental Earth's crust (Favero and Jobstraibizer 1996; Taylor and McLennan 1995, 2009) are possibly due to the piezonuclear fission reactions (1, 2) expressed above (Carpinteri and Manuello 2010). In addition, considering the mass percentage concentrations of other chemical elements, such as Na (∼2.9%), Ni (∼0.01%) and Co (0.003%), in the continental crust (Favero and Jobstraibizer 1996; Taylor and McLennan 1995, 2009; Anbar 2008; Fowler 2005; Doglioni 2007; Rudnick and Fountain 1995), it is possible to conjecture additional piezonuclear fission reactions that could have taken place in correspondence to plate collision and subduction (Carpinteri and Manuello 2010):

$$\mathrm{Co}_{27}^{59} \rightarrow \mathrm{Al}_{13}^{27} + \mathrm{Si}_{14}^{28} + 4 \text{ neutrons}, \quad (3)$$

$$\mathrm{Ni}_{28}^{59} \rightarrow 2\mathrm{Si}_{14}^{28} + 3 \text{ neutrons}, \quad (4)$$

$$\mathrm{Ni}_{28}^{59} \rightarrow \mathrm{Na}_{11}^{23} + \mathrm{Cl}_{17}^{35} + 1 \text{ neutron}. \quad (5)$$

The large concentrations of granite minerals, such as quartz and feldspar (SiO_2, Al_2O_3) in the Earth's crust, and to a lesser extent of magnesite, halite, and zeolite (MgO,

Na_2O, Cl_2O_3), and the low concentrations of magnetite, hematite, bunsenite, and cobaltite minerals (composed predominantly of Fe, Co, and Ni molecules), could be ascribed to piezonuclear reactions (1, 2, 3, 4, 5) due to tectonic and subduction phenomena (Carpinteri and Manuello 2010).

7 Heterogeneity in the Composition of The Earth's Crust: Fe and Al Reservoir Localizations

The localization of Al and Fe mineral reservoirs seems to be closely connected to the geological periods when different continental zones were formed (Favero and Jobstraibizer 1996; Taylor and McLennan 1995, 2009; Anbar 2008; Roy et al. 2001; World Iron Ore producers 2009; World Mineral Resources Map 2009; Key Iron Deposits of the World 2002). This fact would seem to suggest that our planet has undergone a continuous evolution from the most ancient geological regions, which currently reflect the continental cores that are rich in Fe reservoirs, to more recent or contemporary areas of the Earth's crust where the concentrations of Si and Al oxides present very high mass percentages (Favero and Jobstraibizer 1996). The main iron reservoir locations (magnetite and hematite mines) are reported in Fig. 11a. The main concentrations of Al oxides and rocky andesitic formations (the Rocky Mountains and the Andes, with a

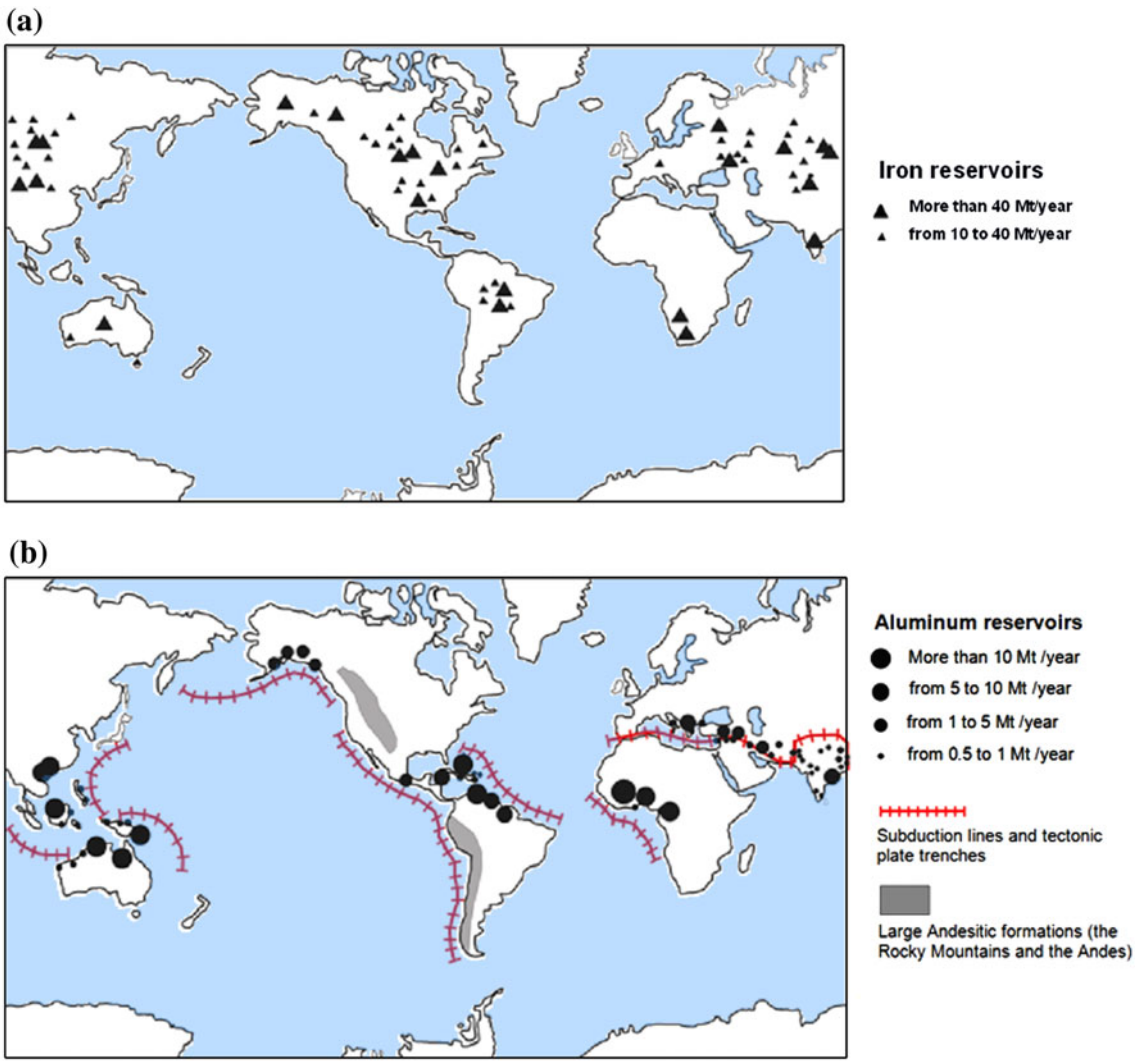

Fig. 11 **a** Locations of the largest iron mines in the world (Roy et al. 2001; World Iron Ore producers 2009; World Mineral Resources Map 2009; Key Iron Deposits of the World 2002). Iron ore reservoirs (magnetite and hematite mines) are located in geographic areas with reduced seismic risks and always far from fault lines. **b** The largest aluminum (bauxite) reservoirs are reported together with the main Andesitic formations and most important subduction lines and plate tectonic trenches (Favero and Jobstraibizer 1996)

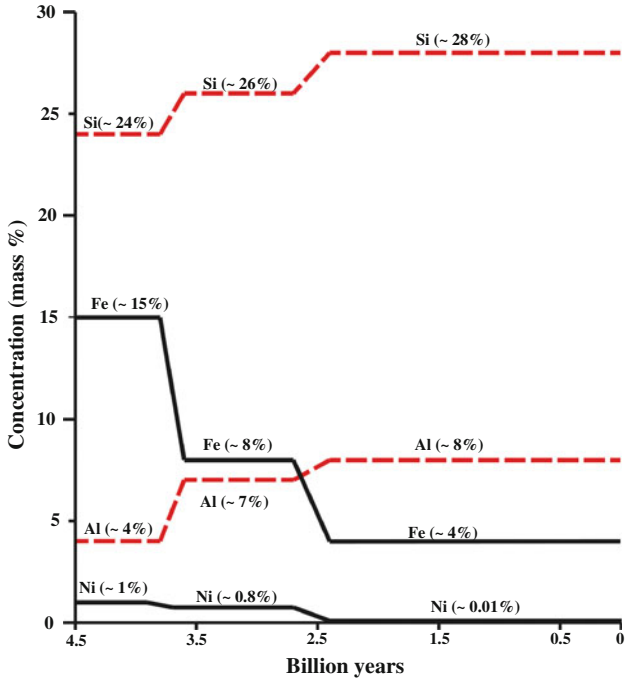

Fig. 12 The estimated concentrations of Fe, Ni, Al, and Si in the Hadean and Archean Earth's protocrust and in the Earth's continental crust are reported. The Archean Earth's protocrust (3.8–2.5 Gyrs ago) had a less basaltic composition (Fe ~ 8%, Ni ~ 0.8%, Al ~ 7%, Si ~ 26%) (Favero and Jobstraibizer 1996; Taylor and McLennan 1995, 2009; Doglioni 2007; Konhauser et al. 2009; Saito 2009; Egami 1975; Natl. Academy of Sciences 1975) compared to the previous period (Hadean Era, 4.5–3.8 Gyrs ago) (Taylor and McLennan 2009; HAzen et al. 2008) and a less Sialic composition compared to the concentrations in the Earth's continental crust today: Fe ~ 4%, Ni ~ 0.01%, Al ~ 8%, Si ~ 28% (Favero and Jobstraibizer 1996; Taylor and McLennan 1995, 2009; Doglioni (2007); Konhauser et al. 2009; Saito 2009; Egami 1975; Natl. Academy of Sciences 1975). Considering piezonuclear reactions (1, 2, 4), the overall 12% decrease in the heavier elements (Fe and Ni) is balanced by the Al and Si increases and assuming an increase in Mg, according to reaction (2), equal to that of Si over the last 4.5 billion years

strong concentration of Al_2O_3 minerals) are shown in Fig. 11b together with the most important subduction lines, plate tectonic trenches, and rifts (Favero and Jobstraibizer 1996; Roy et al. 2001). The geographical locations of main bauxite mines show that the largest concentrations of Al reservoirs can be found in correspondence to the most seismic areas of the Earth (Fig. 11b). The main iron mines are instead exclusively located in the oldest and interior parts of continents (formed through the eruptive activity of the proto-Earth), in geographic areas with a reduced seismic risk and always far from the main fault lines. From this point of view, the close correlation between bauxite and andesitic reservoirs and the subduction and most seismic areas of the Earth's crust provides very impressive evidence of piezonuclear effects at the planetary scale.

8 Geochemical Evidence of Piezonuclear Reactions in the Evolution of The Earth's Crust

Evidence of piezonuclear reactions can be also recognized considering the Earth's composition and its way of evolving throughout the geologic eras. In this way, plate tectonics and the connected plate collision and subduction phenomena are useful to understand not only the morphology of our planet, but also its compositional evolution (Carpinteri and Manuello 2010).

From 4.0 to 2.0 Gyrs ago, Fe could be considered to be one of the most common bio-essential elements required for the metabolic action of all living organisms (Lunine 1998; Hazen et al. 2008; Condie 1976; Canfiled 1998; Holland 2006; Kholodov and Butuzova 2008; Foing 2005; Sigman et al. 2004; Galimov 2005; Yamaguchi 2005). Today, the deficiency of this nutrient suggests it as a limiting factor for the development of marine phytoplankton and life on Earth (Anbar 2008; Canfiled 1998).

Elements such as Fe and Ni in the Earth's protocrust had higher concentrations in the Hadean (4.5–3.8 Gyr ago) and Archean (3.8–2.5 Gyr ago) periods compared to the present values (Taylor and McLennan 1995, 2009; Canfiled 1998; Holland 2006; Basile-Doelsch 2006; Basile-Doelsch et al. 2005; De la Rocha et al. 2000; Ragueneau et al. 2000). The Si and Al concentrations instead were lower than they are today (Favero and Jobstraibizer 1996; Taylor and McLennan 1995, 2009).

The estimated concentrations of Fe, Ni, Al, and Si in the Hadean and Archean Earth's protocrust and in the Earth's continental crust are reported in Fig. 12. The data for the Hadean period (4.5–3.8 Gyrs ago) are referred to the composition of the Earth's protocrust, considering the assumptions made by Foing (2005) and by Taylor and Mclennan (1995, 2009). According to these authors, the Mars and Moon's crusts are considered to be representative of the composition of the early Earth's protocrust (Hadean Eon) (Taylor and McLennan 1995, 2009; Foing 2005).

In the same figure, for the Archean period (3.8–2.5 Gyrs ago) the data are referred to compositional analysis of Archean sediments (Carpinteri and Manuello 2010; Favero and Jobstraibizer 1996; Taylor and McLennan 1995, 2009; Rudnick and Fountain 1995; Konhauser et al. 2009; Saito 2009; Egami 1975). For the last period from 2.5 Gyrs ago to today, the mass percentage concentrations of Fe, Ni, Al, and Si are referred to the present composition of Earth's continental crust (Carpinteri and Manuello 2010; Favero and Jobstraibizer 1996; Taylor and McLennan 1995, 2009; Natl. Academy of Sciences 1975; Yaroshevsky 2006).

A clear transition from a more basaltic condition (high concentrations of Fe and Ni) to a Sialic one (high concentrations of Al and Si) can be observed during the lifetime of our planet (Favero and Jobstraibizer 1996; Taylor

and McLennan 1995, 2009; Doglioni 2007; Rudnick and Fountain 1995; Sigman et al. 2004; Galimov 2005; Yamaguchi 2005; Basile-Doelsch 2006; Basile-Doelsch et al. 2005; De la Rocha et al. 2000; Ragueneau et al. 2000; Konhauser et al. 2009; Saito 2009; Egami 1975; Natl. Academy of Sciences 1975; Yaroshevsky 2006).

The most abrupt changes in element concentrations shown in Fig. 12 appear to be intimately connected to the tectonic activity of the Earth. The vertical drops in the concentrations of Fe and Ni, as well as the vertical jumps in the concentrations of Si and Al, 3.8 Gyrs ago, coincide with the time that many scientists have pointed out as the beginning of tectonic activity on the Earth. The subsequent abrupt transitions 2.5 Gyrs ago coincide with the period of the Earth's largest tectonic activity (Taylor and McLennan 1995, 2009).

As shown in Fig. 12, the decrease in the mass concentration of iron and nickel is balanced by Al and Si increases and assuming an increase in Mg, according to reaction (2), equal to that of Si over the Earth's lifetime. In the same figure, a total decrease of ~7% in Fe and Ni concentrations and a relative increase of ~7% in the lighter chemical element concentrations (Si, Mg and Al) between the Hadean period (Hadean Eon, 4.5–3.8 Gyrs ago) and the Archean period (Archean Eon, 3.8–2.5 Gyrs ago) is shown. Similarly, a decrease of ~5% in the heavier elements (Fe and Ni) and a related increase (~5%) in the concentrations of lighter ones (Si, Mg and Al) can be considered between the Archean period (Archean Eon, 3.8–2.5 billion years ago) and more recent times (Fig. 12). The Earth's protocrust in the Hadean era was strongly basaltic, with a composition similar to that of the proto-planets (chondrites) (Taylor and McLennan 1995, 2009; Condie 1976).

In particular, piezonuclear reactions (1, 2, 4) seem to be the cause of the abrupt variations shown in Fig. 12. Piezonuclear reaction (2) implies that not only the Si mass percentage should increase overall by about 3.5%, but also that of Mg. However, the latter increase, due to piezonuclear reaction (2), cannot be revealed from geological data of sediments in the Earth's continental crust. The most probable explanation is that Mg is not only a resulting element, as shown by piezonuclear reaction (2), but can also be considered as a starting element of another possible piezonuclear reaction (Carpinteri and Manuello 2010):

$$Mg_{12}^{24} \rightarrow 2C_{6}^{12}. \quad (6)$$

Reaction (6) could be very important for the evolution of both the Earth's crust and the atmosphere, and considered as a valid explanation for the high level of CO_2 concentration (~15%) in the Archean Earth's atmosphere (Liu 2007). In addition, the large amount of C produced by Mg transformation (~3.5% of the Earth's crust) has undergone a slow but continuous diminishing in the CO_2 composition of the Earth's atmosphere, as a result of the escape which also involves other atmospheric gases like He and H (Catling and Zahnle 2009).

Piezonuclear reaction (6) can also be correlated with the increase in seismic activity that has occurred over the last century (Aki 1983). Very recent evidence has shown CO_2 emissions in correspondence to seismic activity (Padron et al. 2008): significant changes in the emission of carbon dioxide were recorded in a geochemical station at El Hierro, in the Canary Islands, before the occurrence of several seismic events during the year 2004. Appreciable precursory CO_2 emissions were observed to start before seismic events of relevant magnitude, and to reach their maximum values some days before the earthquakes (Padron et al. 2008).

Relation (6) is not the only piezonuclear reaction that involves Mg as a starting element. Like the considerations made for the concentrations of elements such as Fe, Ni, Al,

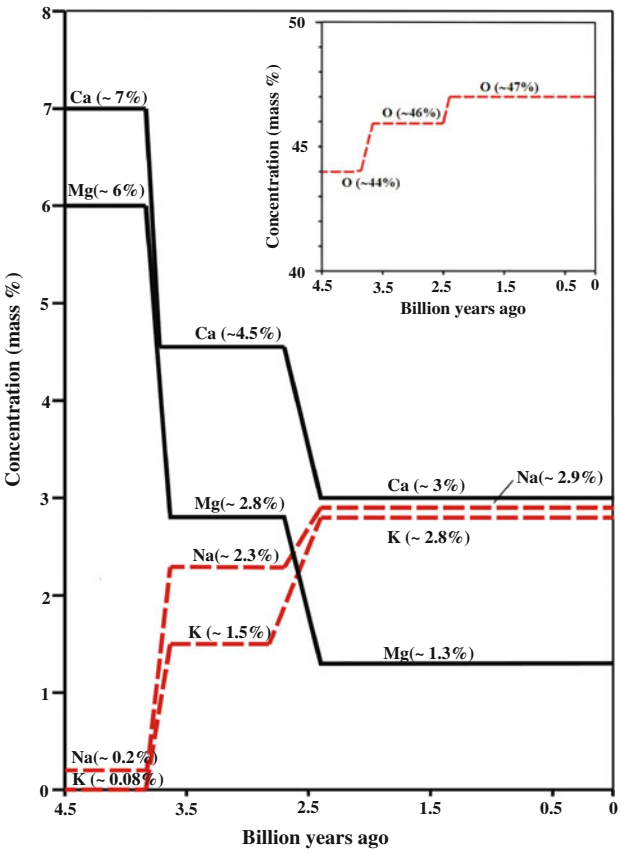

Fig. 13 The variations in mass percentage concentration for Mg, Ca, Na, K, and O in the Hadean and Archean Earth's protocrust and in the Earth's continental crust are reported. It can be noted in particular that the overall 8.7% decrease in alkaline-earth metals (Mg and Ca) is balanced by the Na, K, and O increase (~8.5%) (Favero and Jobstraibizer 1996; Taylor and McLennan 1995, 2009; Yaroshevsky 2006)

and Si (Fig. 12), it is also possible to consider other elements such as Mg, Ca, Na, K, and O, which are involved in other piezonuclear reactions that have been assumed to occur in the chemical evolution of the Earth's crust.

The variations in mass percentage concentration for Mg, Ca, Na, K, and O in the Hadean and Archean Earth's protocrust and in the Earth's continental crust are reported in Fig. 13, analogously to Fig. 12 (Carpinteri and Manuello 2010; Favero and Jobstraibizer 1996; Taylor and McLennan 1995, 2009; Yaroshevsky 2006). The decrease in the mass concentrations of Mg and Ca has been balanced by an increase in Na, K, and O, during the Earth's lifetime. In particular, between the Hadean (4.5–3.8 Gyr ago) and the Archean era (3.8–2.5 Gyrs ago), and between the latter and more recent times, it is possible to observe an overall decrease of $\sim$4.7% for Mg and $\sim$4% for Ca. This decrease in the two alkaline-earth metals (Mg and Ca) seems to be nearly perfectly balanced by the increase in the concentrations of the two alkaline metals, Na and K (which have increased by 2.7 and 2.8%, respectively), and by a total increase ($\sim$3%) in O, which has varied from $\sim$44 to 47% (the latter being the present oxygen concentration in the Earth's crust) (Fig. 13).

9 Conclusions

Neutron emission measurements were performed on Luserna Stone specimens during mechanical tests. From these experiments, it can be clearly seen that piezonuclear reactions giving rise to neutron emissions are possible in inert non-radioactive solids under loading. In particular, during compression tests of specimens with sufficiently large size, the neutron flux was found to be of about one order of magnitude higher than the background level at the time of catastrophic failure. For test specimens with more ductile behavior, neutron emissions significantly higher than the background were found. Neutron detection is also confirmed in compression test under cyclic loading and during ultrasonic vibration.

Our conjecture, also confirmed by the EDS tests, is that piezonuclear reactions involving fission of iron into aluminum, or into magnesium and silicon, should have occurred during compression on the tested specimens.

This hypothesis seems to find surprising evidence and confirmation at the Earth crust scale from both geomechanical and geochemical points of view. In this way, the piezonuclear reactions have been considered to interpret the most significant geophysical and geological transformations, still unexplained to date.

Finally, through experimental and theoretical studies of neutron emission and piezonuclear fission reactions from brittle fracture, it will also be possible to explore new and interesting application fields, such as short-term prediction and monitoring of earthquakes.

Acknowledgments The financial support provided by the Regione Piemonte (Italy) RE-FRESCOS Project is gratefully acknowledged. Special thanks are due to R. Sandrone and A. Chiodoni of the Politecnico di Torino for their kind collaboration in the EDS analysis. The authors wish to thank also D. Madonna Ripa and A. Troia from the National Research Institute of Metrology—INRIM, for their indispensable assistance during the ultrasonic tests.

References

Aki K (1983) Strong motion seismology. In: Kanamori H and Boschi E (eds.) Earthquakes: observation, theory and interpretation, North-Holland Pub. Co., Amsterdam

Anbar AD (2008) Elements and evolution. Science 322:1481–1482

Basile-Doelsch I (2006) Si stable isotope in the Earth's surface: a review. J Geochem Expl 88:252–256

Basile-Doelsch I, Meunier JD, Parron C (2005) Another continental pool in the terrestrial silicon cycle. Nature 433:399–402

Bubble Technology Industries (1992) Instruction manual for the Bubble detector, Copyright Bubble Technology Industries, Chalk River, Ontario

Canfiled DE (1998) A new model for Proterozoic ocean chemistry. Nature 396:450–453

Cardone F, Mignani R (2004) Energy and geometry, Chap. 10. World Scientific, Singapore

Cardone F, Mignani R (2006) Piezonuclear reactions and Lorentz invariance breakdown. Int J Mod Phys E Nucl Phys 15:911–924

Cardone F, Mignani R (2007) Deformed spacetime, Chaps. 16–17. Springer, Dordrecht

Cardone F, Carpinteri A, Lacidogna G (2009a) Piezonuclear neutrons from fracturing of inert solids. Phys Lett A 373:4158–4163

Cardone F, Cherubini G, Petrucci A (2009b) Piezonuclear neutrons. Phys Lett A 373:862–866

Carpinteri A (1989) Cusp catastrophe interpretation of fracture instability. J Mech Phys Solid 37:567–582

Carpinteri A (1990) A catastrophe theory approach to fracture mechanics. Int J Fract 44:57–69

Carpinteri A, Manuello A (2010) Geomechanical and geochemical evidence of piezonuclear fission reactions in the Earth's crust. Strain. doi:10.1111/j.1475-1305.2010.00766.x

Carpinteri A, Cardone F, Lacidogna G (2009) Piezonuclear neutrons from brittle fracture: early results of mechanical compression tests. Strain 45:332–339. Presented at the Turin Academy of Sciences on December 10, 2008. Proc of the Turin Academy of Sciences, Ser. V, 2010 33, 27–42

Carpinteri A, Cardone F, Lacidogna G (2010a) Energy emissions from failure phenomena: mechanical, electromagnetic, nuclear. Exp Mech 50:1235–1243

Carpinteri A, Borla O, Lacidogna G, Manuello A (2010b) Neutron emissions in brittle rocks during compression tests: monotonic vs cyclic loading. Phys Mesomech 13:268–274

Carpinteri A, Chiodoni A, Manuello A, Sandrone R (2010c) Compositional and microchemical evidence of piezonuclear fission reactions in rock specimens subjected to compression tests. Strain. doi:10.1111/j.1475-1305.2010.00767.x

Carpinteri A, Lacidogna G, Manuello A and Borla O (2011) Energy emissions from brittle fracture: neutron measurements and geological evidences of piezonuclear reactions. Strenght Fract Complex. doi:10.3233/SFC-2011-0120

Catling CD, Zahnle KJ (2009) The planetary air leak. Sci Am 300(5):24–31

Compagnoni R, Crisci GM, Sandrone R (1983) Caratterizzazione chimica e petrografica degli''gneiss di Luserna'' (Massiccio cristallino Dora-Maira, Alpi Occidentali) *Rend*. Soc It Min Petr 38:498

Condie KC (1976) Plate Tectonics and crustal evolution. Pergamon Press, New York

De la Rocha CL, Brzezinski M, De Niro MJ (2000) A first look at the distribution of the stable isotopes of silicon in natural waters. Geochim et Cosmochim Acta 64(14):2467–2477

Doglioni C (2007) Interno della Terra, Treccani. Enciclopedia Scienza e Tecnica 595–605

Egami F (1975) Minor elements and evolution. J Mol Evol 4(2):113–120

Favero G, Jobstraibizer P (1996) The distribution of aluminum in the Earth: from cosmogenesis to Sial evolution. Coord Chem Rev 149:400–467

Foing B (2005) Earth's childhood attic. Astrobiological Magazine: Retrospection (on-line)

Fowler CMR (2005) The solid Earth: an introduction to global geophysics. Cambridge University Press, Cambridge

Galimov EM (2005) Redox evolution of the Earth caused by a multistage formation of its core. Earth Planet Sci Lett 233: 263–276

Hazen et al (2008) Mineral evolution. Am Miner 93:1693–1720

Holland HD (2006) The oxygenation of the atmosphere and oceans. Philos Trans R Soc London Ser B 361:903–915

Key Iron Deposits of the World. Available at http://www.portergeo.com.au/tours/iron2002/-iron2002depm2b.asp; last accessed October (2009)

Kholodov VN, Butuzova GY (2008) Siderite formation and evolution on sedimentary iron ore deposition in the Earth's history. Geol Ore Depos 50(4):299–319

Konhauser KO et al (2009) Oceanic nickel depletion and a methanogen famine before the Great Oxidation Event. Nature 458:750–754

Kuzhevskij BM, Nechaev YO, Sigaeva EA, Zakharov VA (2003a) Neutron flux variations near the Earth's crust. A possible tectonic activity detection. Nat Hazards Earth Sys Sci 3:637–645

Kuzhevskij BM, Nechaev YO, Sigaeva EA (2003b) Distribution of neutrons near the Earth's surface. Nat Hazards Earth Sys Sci 3:255–262

Liu L (2007) The inception of the oceans and CO_2-atmosphere in the early history of the Earth. Earth Planet Sci Lett 227:179–184

Lunine EJI (1998) Earth: evolution of a habitable world. Cambridge University Press, Melbourne

National Council on Radiation Protection and Measurements (1971) Protection Against Neutron Radiation, NCRP Report 38

Natl Academy of Sciences (1975) Medical and biological effects of environmental pollutants: Nickel. Proc Natl Acad Sci, Washington D.C.

Padron E, Melian G, Marrero R, Nolasco D, Barrancos J, Padilla G, Hernandez PA, Perez NM (2008) Changes in the diffuse CO_2 emission and relation to seismic activity in and around El Hierro, Canary Islands. Pure Appl Geophys 165:95–114

Ragueneau O et al (2000) A review of the Si cycle in the modern ocean: recent progress and missing gaps in the application of biogenic opal as a paleoproductivity proxy. Global Planet Change 26:317–365

Roy I, Sarkar BC, Chattopadhyay A (2001) MINFO-a prototype mineral information database for iron ore resourcers of India. Comp Geosci 27:357–361

Rudnick RL, Fountain DM (1995) Nature and composition of the continental crust: a lower crustal perspective. Rev Geophys 33(3):267–309

Saito MA (2009) Less nickel for more oxygen. Nature 458:714–715

Sandrone R, Cadoppi P, Sacchi R, Vialon P (1993) The Dora-Maira Massif. In: Von Raumer JF, Neubauer F (eds) Pre-Mesozoic geology in the Alps. Springer, Berlin, pp 317–325

Sandrone R, Colombo A, Fiora L, Fornaro M, Lovera E, Tunesi A, Cavallo A (2004) Contemporary natural stones from the Italian western Alps (Piedmont and Aosta Valley regions). Period Miner (Special issue) 73:211–226

Sigman D, Jaccard S, Hau F (2004) Polar ocean stratification in a cold climate. Nature 428:59–63

Taylor SR, McLennan SM (1995) The geochemical evolution of the continental crust. Rev Geophys 33(2):241–265

Taylor SR, McLennan SM (2009) Planetary crusts: their composition, origin and evolution. Cambridge University Press, Cambridge

Vola G, Marchi M (2010) Quantitative phase analysis (QPA) of the Luserna Stone. Period Miner 79(2):45–60

Volodichev NN, Kuzhevskij BM, Nechaev OYu, Panasyuk MI, Podorolsky A, Shavrin PI (2000) Sun–Moon–Earth connections: the neutron intensity splashes and seismic activity. Astrons Vestnik 34(2):188–190

World Iron Ore producers. Available at http://www.mapsofworld.com/minerals/world-iron-ore-producers.html; last accessed October (2009)

World Mineral Resources Map. Available at http://www.mapsofworld.com/world-mineral-map.htm; last accessed October (2009)

Yamaguchi KE (2005) Evolution of the geochemical cycle of Fe trough geological time: Iron isotope perspective. Frontier Res Earth Evol 2:4–24

Yaroshevsky AA (2006) Abundances of chemical elements in the Earth's crust. Geochem Int 44(1):54–62